Vacuum electron acceleration by coherent dipole radiation

A. L. Troha,[1,2] J. R. Van Meter,[1,2] E. C. Landahl,[1,2] R. M. Alvis,[1,2] Z. A. Unterberg,[3] K. Li,[2] N. C. Luhmann, Jr.,[2] A. K. Kerman,[4] and F. V. Hartemann[1,2]

[1]*Institute for Laser Science and Applications, Lawrence Livermore National Laboratory, Livermore, California 94550*

[2]*Department of Applied Science, University of California, Davis, California 95616*

[3]*Nuclear Engineering Department, University of Tennessee, Knoxville, Tennessee 37916*

[4]*Physics Department and Center for Theoretical Physics, Massachusetts Institute of Technology, Cambridge, Massachusetts 02139*

(Received 11 September 1998)

The validity of the concept of laser-driven vacuum acceleration has been questioned, based on an extrapolation of the well-known Lawson-Woodward theorem, which stipulates that plane electromagnetic waves cannot accelerate charged particles in vacuum. To formally demonstrate that electrons can indeed be accelerated in vacuum by focusing or diffracting electromagnetic waves, the interaction between a point charge and coherent dipole radiation is studied in detail. The corresponding four-potential exactly satisfies both Maxwell's equations and the Lorentz gauge condition everywhere, and is analytically tractable. It is found that in the far-field region, where the field distribution closely approximates that of a plane wave, we recover the Lawson-Woodward result, while net acceleration is obtained in the near-field region. The scaling of the energy gain with wave-front curvature and wave amplitude is studied systematically. [S1063-651X(99)00507-3]

PACS number(s): 41.75.Ht, 41.20.−q, 42.25.Bs, 52.40.Nk

I. INTRODUCTION

In recent years, there has been a growing interest in the possibility of using ultrashort-pulse, table-top terawatt (T^3) lasers [1–3] to accelerate electrons to relativistic energies in vacuum, with extremely high gradients. The concept of laser-driven vacuum acceleration is based on the very high electric fields present at the focus of T^3 lasers, which can reach a few TV/m for intensities exceeding $10^{17}\,W/cm^2$ at visible wavelengths. Preliminary experiments [4,5], based on ponderomotive scattering [6,7], have demonstrated the production of relativistic electrons over small interaction lengths.

There remains, however, an open question regarding the exact origin and scaling of this acceleration mechanism [8–10]. The foundation of this argument is based on an extrapolation of the well-known Lawson-Woodward (LW) theorem, which is presented in a very clear manner in the Introduction of Ref. [11]. Reference [11] also contains a detailed discussion of the dynamics of ultrarelativistic electrons with a laser field in vacuum. The LW theorem essentially stipulates that plane electromagnetic waves cannot accelerate charged particles in vacuum. Within this context, a detailed understanding of the transition from the plane wave to the focusing or diffracting wave geometries (with wave-front curvature and axial electromagnetic field components) is critical in elucidating this question. In particular, because the acceleration mechanism is not a zeroth-order process, but rather relies on the somewhat subtle effects mentioned above, it is extremely important to carefully model the electromagnetic field distribution with which the charged particle is interacting. This was a strong motivation in our previous work [7], where the paraxial propagator formalism was used to model the electromagnetic field of a focused laser pulse. However, such Gaussian models using the paraxial ray approximation have been criticized because the predicted electron acceleration might be attributed to their deviation from Maxwell's equations and the gauge condition. By contrast, in the present work, we are using coherent dipole radiation to study the effects of wave-front curvature on the electron dynamics in a completely rigorous manner. Here, it is crucial to note that the dipole four-vector potential exactly satisfies both Maxwell's equations and the Lorentz gauge condition everywhere, and is analytically tractable; thus, this theoretical model is entirely self-contained, and sufficient to answer the main question raised here.

In this paper, we present detailed results of numerical simulations which demonstrate that electrons are indeed accelerated in vacuum by the coherent radiation from an oscillating electric dipole. As mentioned above, both Maxwell's equations and the Lorentz gauge condition are satisfied, and there are no Coulomb-like electrostatic field components associated with this model, as the dipole has zero net charge; hence, any resultant acceleration must be due to ponderomotive forces. The fields also satisfy two important limits: in the vicinity of the dipole, the fields are similar to those of a diffracting laser pulse near focus; in the far-field region, the fields tend to the plane-wave limit. Thus, one can study the transition from the regime where the LW theorem applies, to the more realistic situation of diffracting dipole radiation and ponderomotive scattering.

This paper is organized as follows: in Sec. II, we briefly review the covariant dynamics of an electron interacting with a plane wave, including the LW theorem and radiative corrections; in Sec. III, we introduce the four-potential of our dipole model, and consider the relativistic equations of motion for an electron subjected to the corresponding electromagnetic field distribution; in Sec. IV, the simulation code is first described and benchmarked against plane wave theory; numerical results from several runs are then analyzed, including the scaling of the energy gain with wave-front curvature and wave amplitude; finally, conclusions are drawn in Sec. V.

II. PLANE WAVE DYNAMICS

This section is intended as a brief review of the interaction of a relativistic electron with a plane wave of arbitrary intensity. For conciseness, we use electron units, where length, time, mass, and charge are measured in units of r_0, r_0/c, m_0, and e, respectively. Here, $r_0=2.8178\times10^{-15}$ m is the classical electron radius; in these units, $\varepsilon_0=1/4\pi$ and $\mu_0=4\pi$. The equation of motion governing the electron dynamics, including radiative recoil is given by the Dirac-Lorentz equation [12–14]

$$a_\mu=\frac{du_\mu}{d\tau}=-F_{\mu\nu}u^\nu+\tau_0\left[\frac{da_\mu}{d\tau}-u_\mu(a_\nu a^\nu)\right], \tag{1}$$

where τ is the proper time along the dimensionless electron world line $x_\mu(\tau)$; $u_\mu(\tau)=dx_\mu/d\tau$ is the four-velocity, which corresponds to the four-momentum in our units; $a_\mu(\tau)=du_\mu/d\tau$ is the four-acceleration; τ_0 is the Compton time scale, which is equal to $\frac{2}{3}$ in electron units, or 0.626×10^{-23} s in MKSA units; and $F_{\mu\nu}=\partial_\mu A_\nu-\partial_\nu A_\mu$ is the electromagnetic field tensor, as defined in terms of the four-potential A_μ.

For plane waves, the four-potential is given by

$$A_\mu(\phi)=[\varphi,\mathbf{A}_\perp(\phi),A_z],\quad \varphi=A_z=0,\quad \phi=k_\mu x^\mu(\tau), \tag{2}$$

where ϕ is the relativistically invariant phase of the traveling wave along the electron trajectory. Note that the temporal dependence of the wave is arbitrary, and that the four-potential satisfies the Lorentz gauge condition, $\partial_\mu A^\mu=0$. Choosing the four-wave number $k_\mu=\varpi_0(1,0,0,1)$, with the wave propagating in the z direction, we have

$$\frac{d\phi}{d\tau}=\varpi_0(\gamma-u_z)=\varpi_0\kappa, \tag{3}$$

which defines the light-cone variable $\kappa=\gamma-u_z$. Here, γ is the normalized electron energy, and $\varpi_0=\omega_0 r_0/c$ is the characteristic pulse frequency, again expressed in electron units.

We first consider the electron dynamics in the absence of radiative corrections; in this case, the Lorentz force equation reads

$$\frac{d\mathbf{u}_\perp}{d\tau}=\varpi_0\kappa\frac{d\mathbf{A}_\perp}{d\phi} \tag{4}$$

and

$$\frac{du_z}{d\tau}=\frac{d\gamma}{d\tau}=\varpi_0\mathbf{u}_\perp\cdot\frac{d\mathbf{A}_\perp}{d\phi}. \tag{5}$$

Equation (5) shows that the light-cone variable is invariant: $\kappa=\kappa_0=\gamma_0(1-\beta_0)$, where γ_0 and β_0 are the initial values of the energy and the axial component of the three-velocity, respectively. Using Eq. (3), and applying the chain rule to the phase derivative in Eq. (4), one readily obtains the transverse momentum invariant, $\mathbf{u}_\perp(\tau)=\mathbf{A}_\perp(\phi)$, where we assume that the perpendicular component of the initial four-velocity is zero. With these two results, and using the fact that $u_\mu u^\mu=-1$, or, equivalently, $\gamma^2=1+u_\perp^2+u_z^2$, the energy and axial momentum are easily derived after some straightforward algebra:

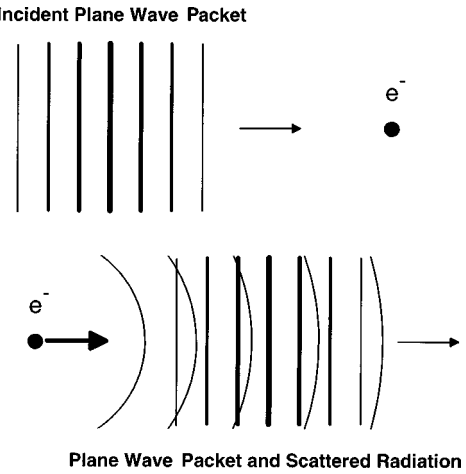

FIG. 1. Initial and final states for the interaction of a plane wave with an electron initially at rest.

$$u_z(\tau)=\gamma_0\left[\beta_0+\frac{\mathbf{A}_\perp^2(\phi)}{2}(1+\beta_0)\right] \tag{6}$$

and

$$\gamma(\tau)=\gamma_0\left[1+\frac{\mathbf{A}_\perp^2(\phi)}{2}(1+\beta_0)\right]. \tag{7}$$

Alternatively, using the relation $\mathbf{u}_\perp(\tau)=\mathbf{A}_\perp(\phi)$, and employing the chain rule in conjunction with Eq. (3), one can rewrite Eq. (5) as $du_z/d\tau=d\gamma/d\tau=(1/2\kappa)d_\tau(\mathbf{A}_\perp^2)$. This is easily integrated, yielding $u_z-u_{z0}=\gamma-\gamma_0=(1/2\kappa)\mathbf{A}_\perp^2$, where u_{z0} is the axial component of the initial normalized four-velocity. Using the invariant value of the light-cone variable, and the relations $u_{z0}=\gamma_0\beta_0$ and $\gamma_0^2=(1-\beta_0^2)^{-1}$, the energy and axial momentum are obtained from this result after a few algebraic manipulations, yielding Eqs. (6) and (7).

These results are quite general and hold as long as plane waves are considered, and radiation reaction effects are neglected. In the relativistic intensity regime, where $\mathbf{A}_\perp^2\gg1$, the axial electron dynamics, which is driven by the ponderomotive force, dominates over the transverse dynamics, which scales linearly with the four-potential. Equation (7) shows that there is no net energy gained by the electron after interacting with a plane wave: we have $\lim_{\phi\to\pm\infty}|\mathbf{A}^\perp(\phi)|=0$, and therefore $\lim_{\phi\to\pm\infty}\gamma(\phi)=\gamma_0$. This is essentially the generalized version of the LW theorem. The fact that a charged particle cannot exchange energy and momentum with an incident plane wave in vacuum can easily be seen by examining the problem in a frame where the electron is initially at rest, as illustrated in Fig. 1. If the electron gains energy and momentum during the interaction, it is accelerated and therefore radiates. In the final state, the plane wave has been attenuated, which implies that there is a permanent destructive interference between the plane wave and the

wave radiated by the electron. This is the classical equivalent of photon annihilation in QED. However, the electron radiates waves which decay like r^{-1} and therefore, no stable interference pattern can be obtained with a plane wave; in fact, in this case, any interference also decays like r^{-1}. This shows that, in the absence of radiative corrections (electron recoil), no net energy momentum can be transferred from a plane wave to an electron in vacuum, in agreement with the generalized LW theorem.

If radiation reaction effects are included, the situation is considerably different; in this case, the Dirac-Lorentz equation now reads [13,14]

$$a_\mu=\frac{du_\mu}{d\tau}=L_\mu+\frac{2}{3}\left[\frac{da_\mu}{d\tau}-u_\mu(a_\nu a^\nu)\right], \tag{8}$$

where $\mathbf{L}_\perp=\kappa\mathbf{E}_\perp$, and $L_z=L_0=\mathbf{u}_\perp\cdot\mathbf{E}_\perp$ corresponds to the Lorentz force. Here, we use the fact that the wave electric field definition, $\mathbf{E}=-\boldsymbol{\nabla}\varphi-\partial_t\mathbf{A}$, reduces to $\mathbf{E}_\perp=\varpi_0 d\mathbf{A}_\perp/d\phi$, for plane waves. Subtracting the axial component of Eq. (8) from the temporal component, one obtains an equation governing the evolution of κ,

$$\frac{d\kappa}{d\tau}=\frac{2}{3}\left[\frac{d^2\kappa}{d\tau^2}-\kappa(a_\nu a^\nu)\right]. \tag{9}$$

Equation (9) is an important result, as it shows that when radiative recoil is taken into account, the light-cone variable is no longer invariant. This, in turn, results in a net energy variation during the electron interaction with a plane wave, as will be shown below; in this case, it is clear that the LW theorem is no longer applicable.

The equation governing the evolution of the transverse momentum is now given by

$$\frac{d}{d\tau}(\mathbf{u}_\perp-\mathbf{A}_\perp)=\frac{2}{3}\left[\frac{d^2\mathbf{u}_\perp}{d\tau^2}-\mathbf{u}_\perp(a_\nu a^\nu)\right]. \tag{10}$$

Introducing the small parameter $\varepsilon=\frac{2}{3}\varpi_0=2\omega_0 r_0/3c$, which essentially measures the pulse wavelength in units of r_0, and using the phase as the independent variable, Eq. (9) can be expressed as

$$\frac{d\kappa}{d\phi}=\varepsilon\left[\frac{d^2}{d\phi^2}\left(\frac{\kappa^2}{2}\right)-\kappa^2\left(\frac{du_\mu}{d\phi}\frac{du^\mu}{d\phi}\right)\right]. \tag{11}$$

To solve Eq. (11), we use perturbation theory, where $\kappa=\kappa^{(0)}+\varepsilon\kappa^{(1)}+\cdots+\varepsilon^n\kappa^{(n)}+\cdots$, and where all other dynamical variables are expressed likewise. Since the right-hand side of Eq. (11) is at least of order ε, we can replace the terms in the brackets by their Lorentz dynamics (zeroth-order) approximation, where $d_\phi\kappa^{(0)}=0$, $d_\phi u_z^{(0)}=d_\phi\gamma^{(0)}$, and $\mathbf{u}_\perp^{(0)}(\phi)=\mathbf{A}_\perp(\phi)$. Thus,

$$\left[\frac{du_\mu}{d\phi}\frac{du^\mu}{d\phi}\right]^{(0)}=\left[\frac{d\mathbf{u}_\perp^{(0)}}{d\phi}\right]^2+\left[\frac{du_z^{(0)}}{d\phi}\right]^2-\left[\frac{d\gamma^{(0)}}{d\phi}\right]^2=\left(\frac{d\mathbf{A}_\perp}{d\phi}\right)^2,$$

which shows that the radiation depends only on the transverse motion, to lowest order. With this, Eq. (11) reduces to $d\kappa/d\phi\simeq-\varepsilon\kappa^2(d\mathbf{A}_\perp/d\phi)^2$. If we consider a circularly polarized plane wave, where the transverse vector potential is described by $\mathbf{A}_\perp(\phi)=A_0 g(\phi)[\hat{x}\sin\phi+\hat{y}\cos\phi]$, and use the slowly varying envelope approximation [i.e., $g(\phi)\gg dg(\phi)/d\phi$], we obtain a simple differential equation for the light-cone variable perturbation:

$$\frac{d}{d\phi}\left[\frac{1}{\kappa(\phi)}\right]\simeq\varepsilon A_0^2 g^2(\phi). \tag{12}$$

Integrating Eq. (12), one obtains

$$\frac{1}{\kappa(\phi)}\simeq\frac{1}{\kappa_0}+\varepsilon A_0^2\int_{-\infty}^{\phi}g^2(\psi)d\psi. \tag{13}$$

This equation describes the recoil of the electron interacting with a circularly polarized plane wave, with a pulse envelope $g(\phi)$. In the case of a hyperbolic secant envelope, where $g(\phi)=\cosh^{-1}(\phi/\Delta\phi)$, Eq. (13) takes the analytical form

$$\frac{1}{\kappa(\phi)}\simeq\frac{1}{\kappa_0}+\varepsilon A_0^2\Delta\phi\left[1+\tanh\left(\frac{\phi}{\Delta\phi}\right)\right], \tag{14}$$

and the fractional variation of the light-cone variable over the entire interaction is

$$\frac{\Delta\kappa}{\kappa_0}\simeq-\frac{2\varepsilon A_0^2\Delta\phi\kappa_0}{1+2\varepsilon A_0^2\Delta\phi\kappa_0}. \tag{15}$$

We can now derive the energy variation during the interaction, using the relation between the light-cone variable and the electron energy,

$$\gamma=\frac{1+\mathbf{u}_\perp^2-\kappa^2}{2\kappa}. \tag{16}$$

Here, we note that $\lim_{\phi\to\pm\infty}\mathbf{u}_\perp^2(\phi)=O(\varepsilon^2)$; this is easily established by considering Eq. (11), which shows that the radiative corrections to the transverse electron dynamics are at least of order ε, and by remembering that there is no electromagnetic wave at $\phi\to\pm\infty$. Using Eq. (16), and assuming that $\Delta\kappa/\kappa_0\ll1$, we find that

$$\Delta\gamma=\gamma_0\beta_0(1-\beta_0)\varepsilon A_0^2\int_{-\infty}^{+\infty}g^2(\phi)d\phi. \tag{17}$$

In the ultrarelativistic limit, for a head-on collision, $\beta_0\to-1$; in the case of a hyperbolic secant pulse, Eq. (17) takes the simple form $\Delta\gamma/\gamma_0\simeq4\gamma_0\varepsilon\Delta\phi A_0^2$.

In summary, it is clear that radiative corrections are beyond the scope of the LW theorem. Radiative energy recoil is seen to scale linearly with the electromagnetic pulse intensity and duration (thus scaling linearly with the pulse energy); also, note that recoil is significant for high-energy Compton backscattering, where the electron loses energy, or when a mildly relativistic electron interacts with high-energy photons ($\lambda\lesssim\lambda\!\!\!^{-}_C=\hbar/m_0c=3.861\times10^{-13}$ m), in which case the electron can gain energy at the expense of the incident radiation field. Radiative corrections are important in some situations, including the recent SLAC nonlinear Compton scattering experiments [13,15], the proposed Linac Coherent Light Source (LCLS) [16], and the γ-γ collider [17]. However, we are interested here in vacuum laser acceleration

using high-intensity, low-frequency (visible) photon fields, where the acceleration process does not rely on radiative corrections, but rather on wave-front curvature and axial electromagnetic field components. This is studied in the next section.

III. ELECTRON DYNAMICS IN A COHERENT DIPOLE FIELD

In this section, radiation reaction effects are not taken into account; therefore, the natural units of length and time are given by the radiation wave packet characteristic wave number k_0^{-1}, and frequency, ω_0^{-1}, respectively. In the case of an idealized oscillating electric dipole, the vector potential takes the form [18]

$$\mathbf{A}(x_\mu)=A_0\frac{f(\phi)}{r}\hat{x}, \tag{18}$$

where $r=\sqrt{x^2+y^2+z^2}$ is the distance from the dipole, $\hat{x}$ is the direction of polarization of the dipole (direction of the oscillating current), $\phi=t-r$ is the radial phase, expressed in normalized units, and $f(\phi)$ is an arbitrary function of the phase which corresponds to the temporal behavior of the dipole current. Without loss of generality, we define $f(\phi)=g(\phi)\cos\phi$, where $g(\phi)$ is the temporal envelope of the dipole oscillatory motion. The scalar potential is obtained from the Lorentz gauge condition, $\partial_\mu A^\mu=0$, with the result that

$$\varphi(x_\mu)=A_0\frac{x}{r^2}\left[\frac{h(\phi)}{r}+f(\phi)\right], \tag{19}$$

where $h(\phi)=\int f(\phi)dt$. At this point, it is important to verify that Maxwell's equations are completely satisfied by this form of the four-potential and the Lorentz gauge condition. The latter is verified by virtue of Eq. (19); also, since we are using the four-potential, with $\mathbf{E}=-\boldsymbol{\nabla}\varphi-\partial_t\mathbf{A}$ and $\mathbf{B}=\boldsymbol{\nabla}\times\mathbf{A}$, Maxwell's source-free equations, $\boldsymbol{\nabla}\cdot\mathbf{B}=0$ and $\boldsymbol{\nabla}\times\mathbf{E}+\partial_t\mathbf{B}=\mathbf{0}$, are automatically satisfied. Therefore, all we need to check is that $\boldsymbol{\nabla}\cdot\mathbf{E}=0$ and $\boldsymbol{\nabla}\times\mathbf{B}-\partial_t\mathbf{E}=\mathbf{0}$, as we are considering the propagation of the dipole wave in vacuum. In terms of the potential, these equations reduce to the wave equation, $\Box A_\mu=[\partial_\nu\partial^\nu]A_\mu=[\nabla^2-\partial_t^2]A_\mu=0$, which is indeed verified by the dipole four-potential, $A_\mu=[\varphi,A_x,0,0]$.

The Lorentz force components can easily be calculated from the four-potential. For the y and z components, this yields

$$\frac{du_y}{d\tau}=-u^\mu\partial_y A_\mu=-\frac{y}{r}(u^\mu\partial_r A_\mu) \tag{20}$$

and

$$\frac{du_z}{d\tau}=-u^\mu\partial_z A_\mu=-\frac{z}{r}(u^\mu\partial_r A_\mu), \tag{21}$$

where we recognize the fact that the partial derivatives operate only on the variable r (when it occurs alone as a spatial variable, and as part of the invariant phase); thus, we can rewrite the derivatives in terms of r, using the chain rule. For the x component, the situation is similar, but we must proceed with care: there are two extra terms in the Minkowski force component along the polarization axis, the first is due to the multiplicative factor of the variable x in the scalar potential, while the second comes from the fact that the vector potential has a component in that direction. Hence, the x component of the Minkowski four-force can be expressed as

$$\frac{du_x}{d\tau}=-(u^\mu\partial_x A_\mu-u^\mu\partial_\mu A_x)=\gamma\frac{\varphi}{x}-\frac{x}{r}u^\mu\partial_r A_\mu+u^\mu\partial_\mu A_x. \tag{22}$$

Finally, the timelike component of the Lorentz force equation governs the evolution of the electron energy, and reads

$$\frac{d\gamma}{d\tau}=-(u^\mu\partial_t A_\mu-u^\mu\partial_\mu\varphi)=u_x\left(\frac{dA_x}{d\phi}+\frac{\varphi}{x}\right)+(\mathbf{u}\cdot\hat{\mathbf{r}})\partial_r\varphi. \tag{23}$$

If one examines Eqs. (20)–(22), an interesting symmetry emerges: all of the spatial components of the Minkowski four-force depend upon a common term, namely $(1/r)u^\mu\partial_r A_\mu$. Thus, one can rearrange the terms in Eqs. (20)–(22) to obtain the following identities:

$$\frac{1}{y}\frac{du_y}{d\tau}=\frac{1}{z}\frac{du_z}{d\tau}=\frac{1}{x}\left(\frac{du_x}{d\tau}-u^\mu\partial_\mu A_x-\gamma\frac{\varphi}{x}\right)=-\frac{1}{r}u^\mu\partial_r A_\mu. \tag{24}$$

These identities are useful in checking the accuracy of the numerical code used to simulate the electron dynamics in the dipole field. The quantity to the right-hand side of Eq. (24) can be expressed explicitly as

$$\begin{aligned}u^\mu\partial_r A_\mu&=u^x\partial_r A_x-\gamma\partial_r\varphi\\&=\frac{A_0}{r}\left\{\gamma\frac{x}{r}\left[\frac{3}{r}\left(\frac{h}{r}+f\right)+\frac{df}{d\phi}\right]\right.\\&\quad\left.-u_x\left(\frac{f}{r}+\frac{df}{d\phi}\right)\right\};\end{aligned} \tag{25}$$

also, we have

$$u^\mu\partial_\mu A_x=[(\mathbf{u}\cdot\boldsymbol{\nabla})+\gamma\partial_t]A_x=\frac{A_0}{r}\left[\gamma\frac{df}{d\phi}-u_r\left(\frac{f}{r}+\frac{df}{d\phi}\right)\right]. \tag{26}$$

The solution to the relativistic equations of motion is not analytically tractable, but in the limiting case where the distance from the dipole, as measured in units of k_0^{-1}, is a large number, we recover the plane wave dynamics discussed in Sec. II. For shorter distances, where the wave-front curvature and the axial electromagnetic field components are significant, a numerical code has been developed, and is presented in Sec. IV. We now derive the electromagnetic field corresponding to the dipole four-potential from the relation $F_{\mu\nu}=\partial_\mu A_\nu-\partial_\nu A_\mu$. The electric field of the ideal oscillating dipole is given by

$$E_x=\frac{A_0}{r}\left\{\left(\frac{x}{r}\right)^2\left[\frac{3}{r}\left(\frac{h}{r}+f\right)+\frac{df}{d\phi}\right]-\left[\frac{1}{r}\left(\frac{h}{r}+f\right)+\frac{df}{d\phi}\right]\right\}, \tag{27}$$

$$E_y=A_0\left(\frac{xy}{r^3}\right)\left[\frac{3}{r}\left(\frac{h}{r}+f\right)+\frac{df}{d\phi}\right], \tag{28}$$

and

$$E_z=A_0\left(\frac{xz}{r^3}\right)\left[\frac{3}{r}\left(\frac{h}{r}+f\right)+\frac{df}{d\phi}\right], \tag{29}$$

while the magnetic induction is given by

$$B_x=0, \tag{30}$$

$$B_y=\frac{A_0}{r}\left(\frac{z}{r}\right)\left[\frac{f}{r}+\frac{df}{d\phi}\right], \tag{31}$$

and

$$B_z=-\frac{A_0}{r}\left(\frac{y}{r}\right)\left[\frac{f}{r}+\frac{df}{d\phi}\right]. \tag{32}$$

In the limit where the distance from the radiating dipole, as measured in units of the characteristic oscillation wavelength $k_0^{-1}=\lambda_0/2\pi$, is large, it is easy to show that the electromagnetic field distribution reduces to that of a plane wave: we have

$$\begin{aligned}E_x&\simeq-\frac{A_0}{r}\left\{\frac{df}{d\phi}\left[1-\left(\frac{x}{r}\right)^2\right]+O(r^{-1})\right\}+O(r^{-3})\\&\simeq-\frac{A_0}{r}\frac{df}{d\phi}\left[1-\left(\frac{x}{r}\right)^2\right],\end{aligned} \tag{33}$$

$$E_y\simeq A_0\left(\frac{xy}{r^3}\right)\frac{df}{d\phi}+O(r^{-4})\simeq 0, \tag{34}$$

and

$$E_z\simeq A_0\left(\frac{xz}{r^3}\right)\frac{df}{d\phi}+O(r^{-4})\simeq 0, \tag{35}$$

for the electric field, and

$$B_x=0, \tag{36}$$

$$B_y\simeq\frac{A_0}{r}\left(\frac{z}{r}\right)\left[\frac{df}{d\phi}+O(r^{-1})\right]\simeq\frac{A_0}{r}\left(\frac{z}{r}\right)\frac{df}{d\phi}, \tag{37}$$

and

$$B_z\simeq-\frac{A_0}{r}\left(\frac{y}{r}\right)\left[\frac{df}{d\phi}+O(r^{-1})\right]\simeq-\frac{A_0}{r}\left(\frac{y}{r}\right)\frac{df}{d\phi}, \tag{38}$$

for the magnetic induction. For $z=r$, we recover the plane wave relation $B_y=E_x$; it is also important to note that in order to compare the dipole field with a plane wave, diffraction must be taken into account by rescaling the amplitude of the four-potential as $A_0\rightarrow A_0/r$. This is consistent as long as the relative displacement along the z axis is small compared to the distance from the dipole, so that diffraction over the interaction length remains negligible.

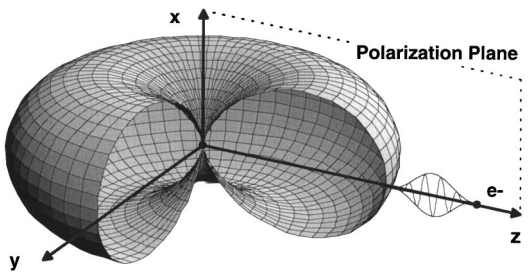

FIG. 2. Dipole intensity distribution, and geometry of the interaction.

Finally, we note that for a linearly polarized dipole wave, as described here, the electron trajectory remains in the plane of polarization; in other words, we can arbitrarily set $y=0$ because of the azimuthal symmetry of the dipole radiation pattern (see Fig. 2), and have $E_y=B_z=0$. Because $B_x=0$ as well, it is clear that there is no component of the Lorentz force in the y direction; as a result, the electron trajectory remains two-dimensional and contained within the x-z (polarization) plane.

According to classical electrodynamic theory, any electromagnetic wave can be described in terms of a multipole expansion [18,19]. The lowest-order moment is the dipole term, which we have employed in our simulations; contributions from quadrupole, octupole, and other higher-order moments will be added to future versions of these simulations in order to provide a full description of a laser focus in vacuum based on a multipole expansion. Vacuum laser acceleration could then be systematically verified for each order of the expansion and studied in detail with an electromagnetic field distribution which fully satisfies Maxwell's equations and the gauge condition.

IV. NUMERICAL SIMULATIONS

The independent variable is chosen to be the radial phase, $\phi=t-r$; the evolution of the four-velocity is then described by

$$\frac{du_\mu}{d\phi}=\frac{du_\mu}{d\tau}\frac{d\tau}{d\phi}=a_\mu(\gamma-u_r)^{-1}, \tag{39}$$

where the four-acceleration, a_μ, is described by Eqs. (20)–(23), and where the radial component of the four-velocity is given by

$$u_r=\frac{dr}{d\tau}=\mathbf{u}\cdot\hat{\mathbf{r}}=\frac{xu_x+yu_y+zu_z}{\sqrt{x^2+y^2+z^2}}. \tag{40}$$

The four-position of the electron is evaluated as

$$x_\mu(\phi)=x_\mu(\phi=0)+\int_0^\phi\frac{dx_\mu}{d\psi}d\psi=x_{\mu 0}+\int_0^\phi\left[\frac{u_\mu}{\gamma-u_r}\right](\psi)d\psi. \tag{41}$$

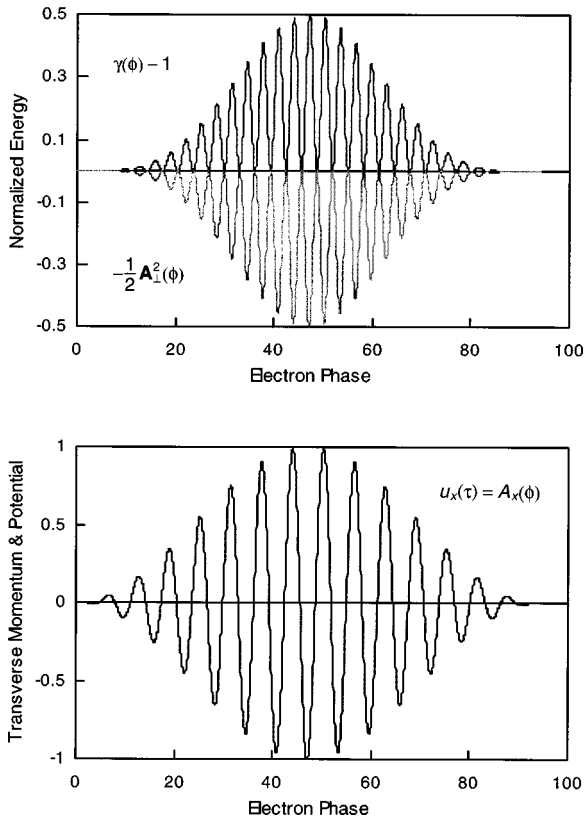

FIG. 3. Top: electron energy as a function of phase, and comparison with the plane wave case. Bottom: transverse momentum and vector potential, in the Lawson-Woodward limit.

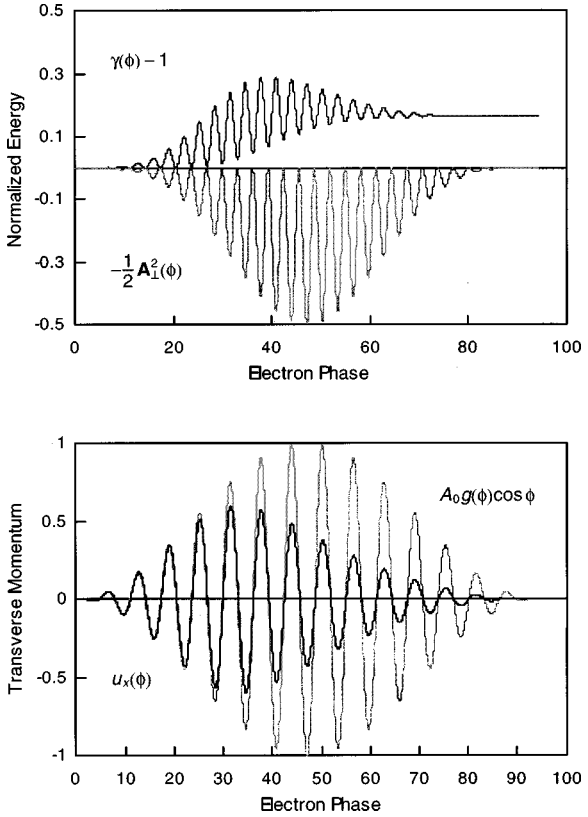

FIG. 4. Top: electron energy as a function of phase, and comparison with the plane wave case. Bottom: transverse momentum and vector potential, in the ponderomotive scattering regime.

In order to increase the accuracy of the code, a second-order Runge-Kutta algorithm is used, where each dynamical variable, $w(\phi)$, is evaluated according to

$$w(\phi+\delta\phi)\simeq w(\phi)+\delta\phi\frac{dw}{d\phi}(\phi)+\frac{\delta\phi^2}{2}\frac{d^2w}{d\phi^2}(\phi). \quad (42)$$

The light-cone variable, $\kappa=\gamma-u_r$, is calculated using the identity $u_\mu u^\mu=-1$, with the result that $\kappa=[1+(\mathbf{u}\times\hat{\mathbf{r}})^2]/(\gamma+u_r)$. Also, the evolution equation for the light-cone variable

$$\frac{d\kappa}{d\phi}=\frac{d}{d\phi}(\gamma-u_r)=\frac{1}{\gamma-u_r}\left[u_x\left(\frac{dA_x}{d\phi}+\frac{\varphi}{x}\right)+u_r\frac{\partial\varphi}{\partial r}-\left(\frac{\mathbf{u}^2-u_r^2}{r}\right)\right]-\hat{\mathbf{r}}\cdot\frac{d\mathbf{u}}{d\phi}, \quad (43)$$

is used to randomize the numerical noise and minimize the growth of numerical instabilities by introducing the averaged quantities

$$\langle\kappa\rangle=\frac{1}{2}\left[\kappa_0+\int_0^\phi\frac{d\kappa}{d\psi}d\psi+\frac{1+(\mathbf{u}\times\hat{\mathbf{r}})^2}{\gamma+u_r}\right] \quad (44)$$

and

$$\langle\gamma\rangle=\frac{1}{2}\left[\gamma_0+\int_0^\phi\frac{d\gamma}{d\psi}d\psi+\sqrt{1+\mathbf{u}^2}\right]. \quad (45)$$

The convergence of the code is verified by comparing alternative calculated values of the energy, namely,

$$\gamma(\phi)=\gamma(\phi=0)+\int_0^\phi\left[\frac{a_0}{\gamma-u_r}\right](\psi)d\psi \quad (46)$$

and

$$\gamma(\phi)=\sqrt{1+u_x^2(\phi)+u_y^2(\phi)+u_z^2(\phi)}. \quad (47)$$

The relative numerical error is obtained by dividing the difference between Eqs. (46) and (47) by the average value of the energy, $\langle\gamma\rangle$.

The code is first benchmarked against plane wave dynamics, as summarized in Sec. II. The initial normalized distance

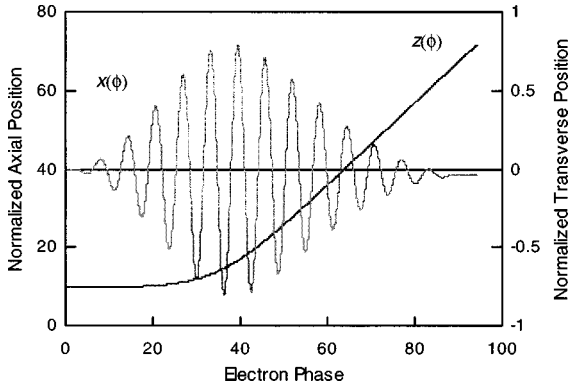

FIG. 5. Typical electron trajectory for ponderomotive scattering.

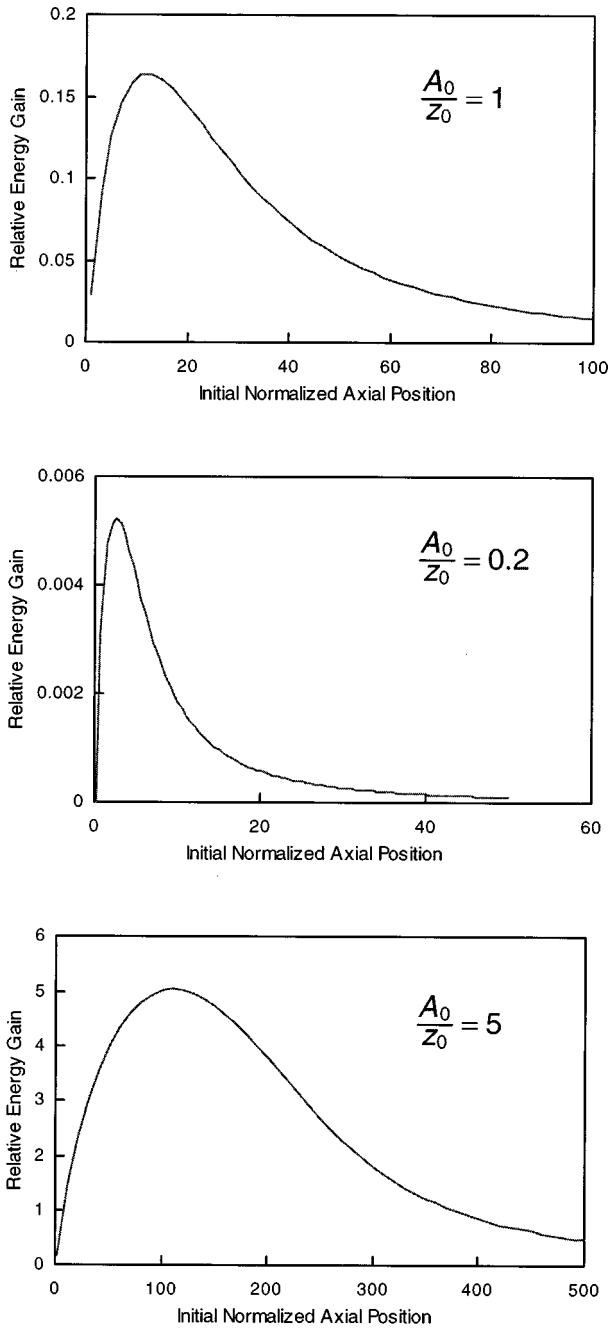

FIG. 6. Scaling of the relative energy gain with the wave-front curvature.

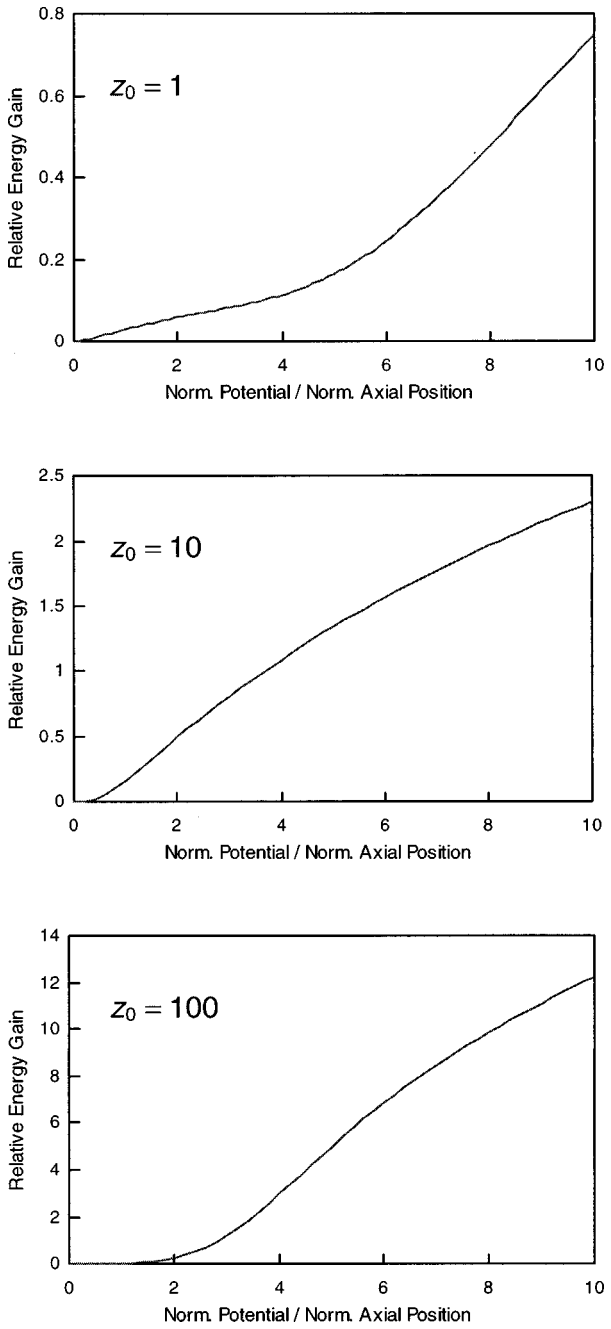

FIG. 7. Scaling of the relative energy gain with the dipole wave amplitude.

from the radiating dipole is set at a large value: $x_0 = y_0 = 0$, $z_0 = 10^6$. The temporal pulse envelope is modeled by the function $g(\phi) = \sin^2(\pi\phi/\omega_0\Delta t) = \sin^2(\pi\phi/\Delta\phi)$ in order to integrate the equations of motion over the finite phase interval $\phi \in [0, \Delta\phi]$; this envelope also closely approximates a Gaussian near its maximum. The dipole parameters consistently used throughout our analysis are: an intensity full width at half maximum (FWHM) of 10 fs, and a wavelength $\lambda_0 = 0.8\,\mu$m, corresponding to the central wavelength of Ti:Al_2O_3 CPA lasers [1–3]. The initial electron energy is chosen to be $\gamma_0 = 1$, with the particle at rest before the interaction; any other case can easily be modeled by boosting the dipole four-potential using the Lorentz transform. Finally, the initial position of the electron along the direction of polarization is chosen to be zero, since the dipole field amplitude is maximized in the x-y plane, as shown in Fig. 2.

The electron energy (top) and transverse momentum along the polarization axis (bottom) are shown as functions of the phase in Fig. 3, and compared to the results obtained for plane waves. In this case, $A_0/z_0 = 1$, for the dipole field, and $A_0 = 1$, for the plane wave. The results fully validate the code accuracy for small wave-front curvatures: the maximum relative difference between the dipole and plane wave models is $< 10^{-10}$. Consequently, these results clearly verify the LW theorem.

A much smaller value of the initial electron position is now considered: $z_0 = 10$. The amplitude of the four-potential is chosen so that $A_0/z_0 = 1$. In this case, shown in

Fig. 4, scattering is obtained, and the electron energy is increased after the interaction. The corresponding electron trajectory is shown in Fig. 5, where we have plotted $x(\phi)$ and $z(\phi)$. The numerical error for this run is quite low ($<10^{-10}$), and many orders of magnitude smaller than the energy gain, thus clearly indicating that the net acceleration results from the dynamics, and that the LW theorem is not applicable for this level of wave-front curvature.

Now, we perform a systematic study of the scaling of the energy gain, $\Delta\gamma=\gamma(\Delta\phi)-\gamma_0=\gamma^*-\gamma_0$, both in terms of the wave-front curvature, and dipole wave amplitude. In the first instance, the initial amplitude of the dipole wave is fixed (A_0/z_0 is held constant), and we run the code for different values of the initial distance from the dipole, z_0. The results are shown in Fig. 6, where we plot the relative energy gain $(\Delta\gamma/\gamma_0)(z_0)$ for three different values of A_0/z_0, namely 0.2, 1.0, and 5. These calculations clearly show the transition between the LW regime, obtained for high values of z_0, and the ponderomotive scattering regime, which corresponds to highly curved wave fronts. Furthermore, we have quantified the variation of the relative energy gain with the wave-front curvature, by fitting the data displayed on a log-log scale to an inverse power law, where $(\Delta\gamma/\gamma_0)(z_0)\propto z_0^{-n}$. It was found that the power n varied between 1.948 and 2.16 for values of A_0/z_0 ranging between 0.1 and 10; therefore, an inverse square scaling appropriately describes the transition from ponderomotive scattering to the LW plane wave regime. This result agrees well with physical intuition, and shows the important role played by the axial electric field component: by inspecting Eq. (35), we see that E_z approximately scales like r^{-2} since $r\simeq z$ at large distances, where the transverse displacement satisfies the inequality $x/r\ll 1$.

In the second case, the initial distance from the dipole is fixed, and we now study the behavior of $(\Delta\gamma/\gamma_0)(A_0/z_0)$, for three different values of z_0: 1, 10, and 100. The results are shown in Fig. 7. Two distinct scattering regimes appear: at low intensities, where the effective normalized potential typically satisfies the relation $A_0/z_0\lesssim 1$, scattering is inefficient and the relative energy gain is small. In contrast, at relativistic intensities, ponderomotive scattering can impart a sizable energy to the electron. Note, however, that this energy gain does not scale like the maximum energy in a plane wave, which increases quadratically with the electromagnetic potential, as shown in Eq. (7); rather, the energy gain appears to be slower than linear, as shown in Fig. 7.

V. CONCLUSIONS

There is a lively debate regarding the exact origin of the mechanism for vacuum acceleration of relativistic electrons by an intense electromagnetic pulse [8–10]. In this paper, we have studied theoretically and numerically the vacuum interaction of an electron with a coherent dipole field distribution exactly satisfying both Maxwell's equations and the Lorentz gauge condition. This is important, because the scattering results obtained cannot be attributed to approximations in the electromagnetic field distribution. It was found that in the limit where the wave-front curvature of the dipole field is small, the electron dynamics predicted by the plane wave theory were recovered, in agreement with the LW theorem: no net energy gain was observed. In the regime where the wave-front curvature is significant, it was found that the LW theorem no longer applies; indeed, net electron acceleration was obtained. We then systematically studied the scaling of the energy gain with the wave amplitude, and with the wave-front curvature. It was found that the wave-front curvature plays a major role in the acceleration mechanism; in addition, two distinct scattering regimes can be defined in terms of the wave intensity: the nonrelativistic intensity regime, where the effective normalized vector potential is much smaller than unity $[(A_0/z_0)^2\ll 1]$ and the energy gain is small, and the relativistic regime, where the axial dynamics dominates over the transverse motion, yielding a quasilinear scaling of the energy gain with A_0/z_0. Finally, it was also shown that when radiation reaction is taken into account, plane waves can exchange energy and momentum with a charged particle, but the effect is essentially nonlinear and scales as the square of the charge and external field, in a regime where the LW theorem clearly no longer applies.

ACKNOWLEDGMENTS

This work was partially supported under the auspices of the U.S. Department of Energy by the Lawrence Livermore National Laboratory under Contract No. W-7405-ENG-48 through the Institute for Laser Science and Applications, and by DoD/AFOSR (MURI) F49620-95-1-0253, AFOSR (ATRI) F30602-94-2-001, and ARO DAAHO4-95-1-0336. One of us (F.V.H.) would also like to personally acknowledge very stimulating conversations with D. T. Santa Maria, while another one of us (A.L.T.) wishes to thank S. O. Nemirovsky for beneficial correspondence.

[1] M. D. Perry and G. Mourou, Science **264**, 917 (1994).
[2] G. A. Mourou, C. P. J. Barty, and M. D. Perry, Phys. Today **51** (1), 22 (1998).
[3] D. P. Umstadter, C. Barty, M. Perry, and G. A. Mourou, Opt. Photonics News **9** (7), 41 (1998).
[4] C. I. Moore, J. P. Knauer, and D. D. Meyerhofer, Phys. Rev. Lett. **74**, 2439 (1995).
[5] G. Malka, E. Lefebvre, and J. L. Miquel, Phys. Rev. Lett. **78**, 3314 (1997).
[6] F. V. Hartemann *et al.*, Phys. Rev. E **51**, 4833 (1995).
[7] F. V. Hartemann *et al.*, Phys. Rev. E **58**, 5001 (1998).
[8] K. T. McDonald, Phys. Rev. Lett. **80**, 1350 (1998).
[9] P. Mora and B. Quesnel, Phys. Rev. Lett. **80**, 1351 (1998).
[10] E. Lefebvre, G. Malka, and J. L. Miquel, Phys. Rev. Lett. **80**, 1352 (1998).
[11] E. Esarey, P. Sprangle, and J. Krall, Phys. Rev. E **52**, 5443 (1995).
[12] P. A. M. Dirac, Proc. R. Soc. London, Ser. A **167**, 148 (1938).
[13] F. V. Hartemann and A. K. Kerman, Phys. Rev. Lett. **76**, 624 (1996).
[14] F. V. Hartemann, Phys. Plasmas **5**, 2037 (1998).
[15] C. Bula *et al.*, Phys. Rev. Lett. **76**, 3116 (1996).

[16] J. Arthur *et al.*, Linac Coherent Light Source (LCLS) Design Study Report, SLAC-R-0521, Stanford Linear Accelerator Center, Stanford (1998). This report is available electronically on the World Wide Web at http://www.slac.stanford.edu/pubs/slacreports/slac-r-521.html.

[17] K. J. Kim and A. Sessler, Beam Line **26 (1)**, 16 (1996). This article is available electronically on the World Wide Web at http://www.slac.stanford.edu/~achim/ps/96i16.pdf.

[18] A. Shadowitz, *The Electromagnetic Field* (Dover, New York, 1975), Chap. 19.

[19] J. D. Jackson, *Classical Electrodynamics*, 2nd ed. (Wiley, New York, 1975), Chap. 16.